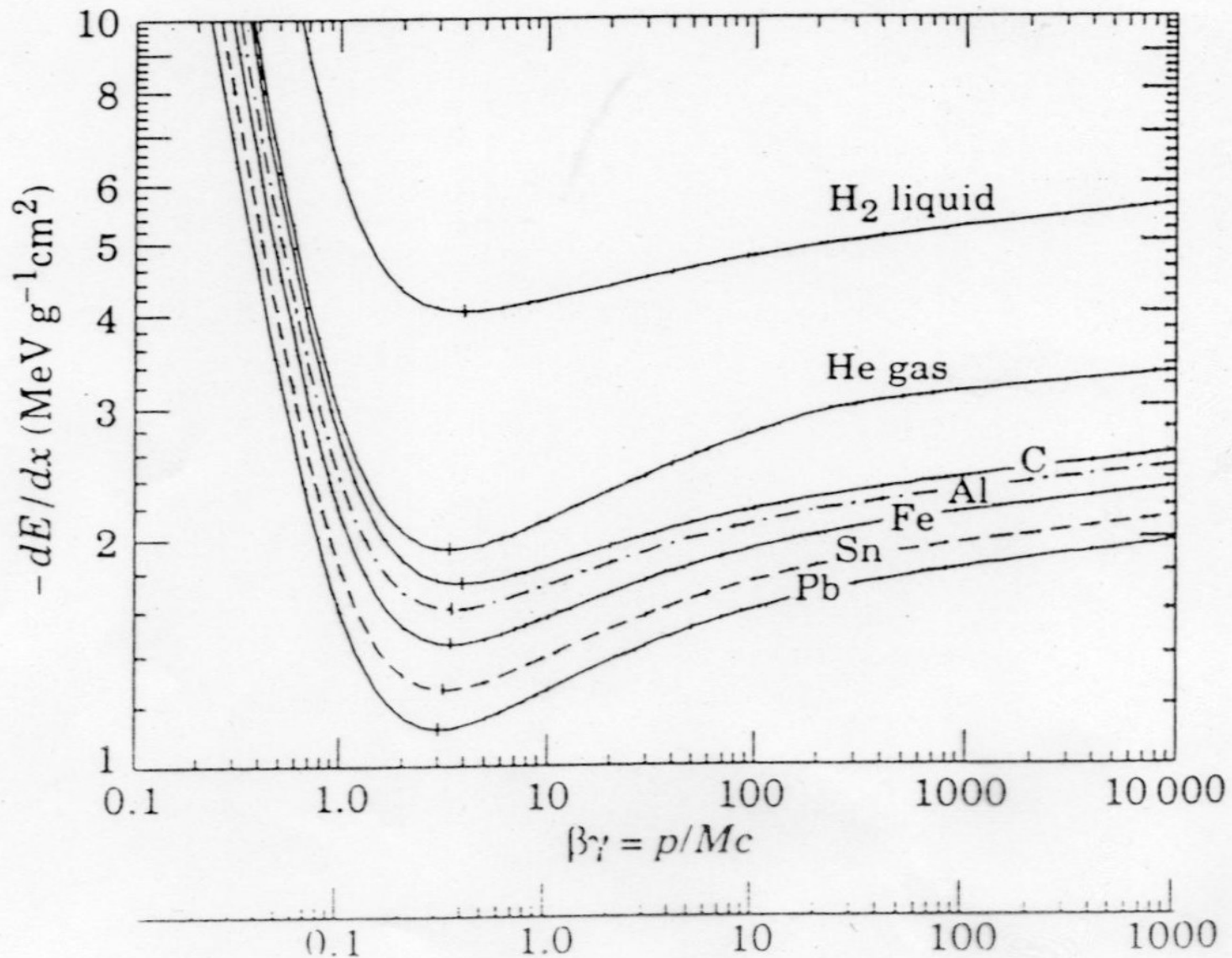
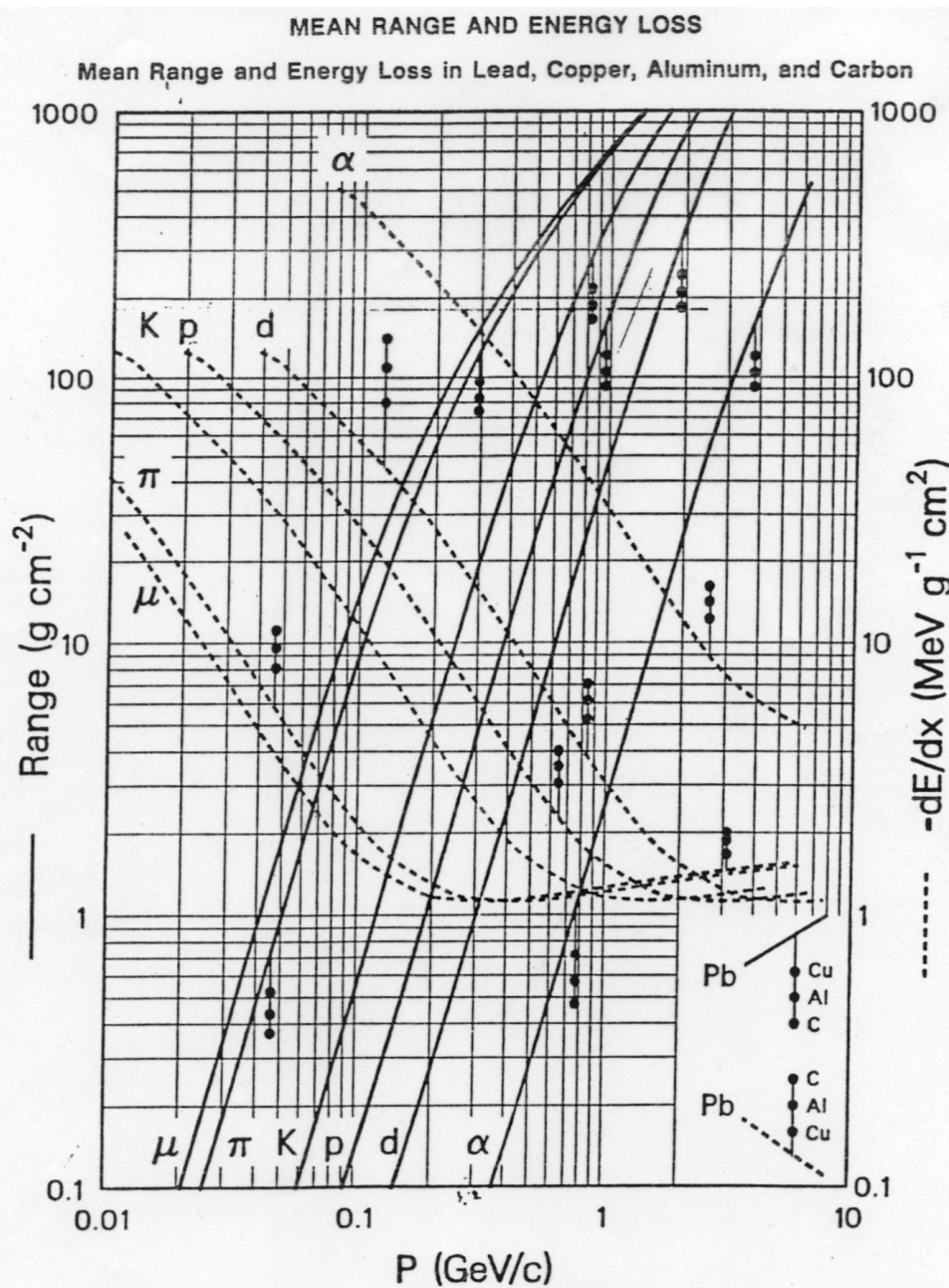


Bemerkung: Plasmaenergie $\propto \sqrt{n}$,
d.h. Dichtekorrektur des relativistischen Anstiegs nach unten groesser in
Fluessigkeiten und Festkoepfern



Energieverlust durch Ionisation (Bethe-Bloch) und Reichweite



Mean range and energy loss due to ionization for the indicated particles in Pb, with scaling to Cu, Al, and C indicated, using Bethe-Bloch equation [See Sec. (I) of Passage of Particles Through Matter] with corrections. Calculated by M.J. Berger, using ionization potentials and density effect corrections as discussed in M.J. Berger and S.M. Seltzer, "Stopping Powers and Ranges of Electrons and Positrons," (2nd ed.), U.S. National Bureau of Standards Report NBSIR 82-2550-A (1982). The average ionization potentials (I) assumed were: Pb (823 eV), Cu (322 eV), Al (166 eV), and C (78.0 eV). Figure indicates total path length; observed range may be smaller (by $\sim 1\%$ - 2% in heavy elements) due to multiple scattering, primarily from small energy-loss collisions with nuclei. The functional forms have not been experimentally verified to better than roughly $\pm 1\%$. For higher energies refer to discussion by Cobb ["A Study of Some Electromagnetic Interactions of High Velocity Particles with Matter," University of Oxford Report HEP/T/55 (1973)] and by Turner ["Penetration of Charged Particles in Matter: A Symposium," National Academy of Sciences, Washington D.C. (1970), p. 48]. For lower energies both data and theory are not well understood. Scaling to other beam particles is, to a good approximation, described by the formula on the next page.

Energieverlust von Elektronen und Positronen

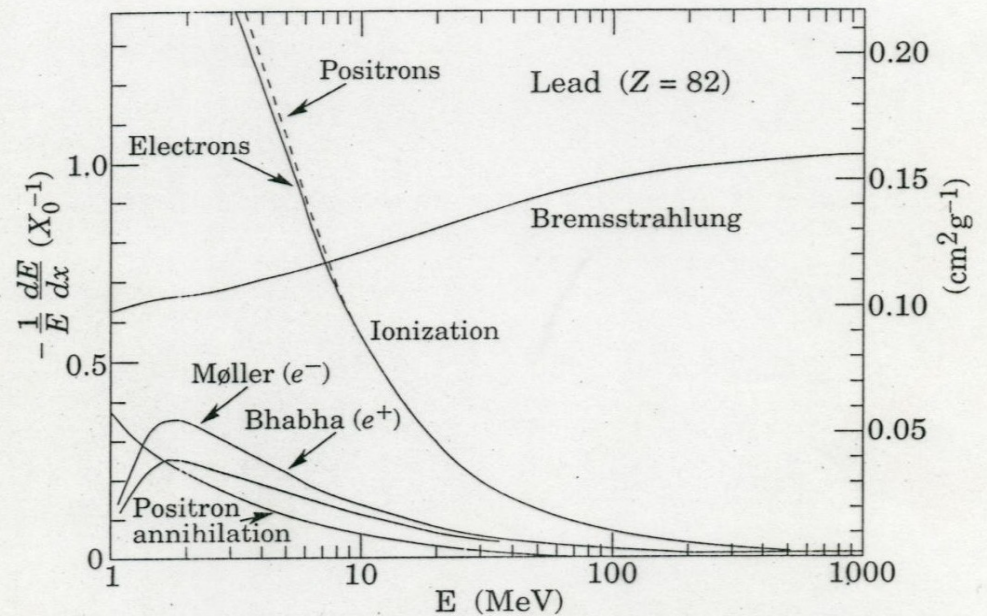
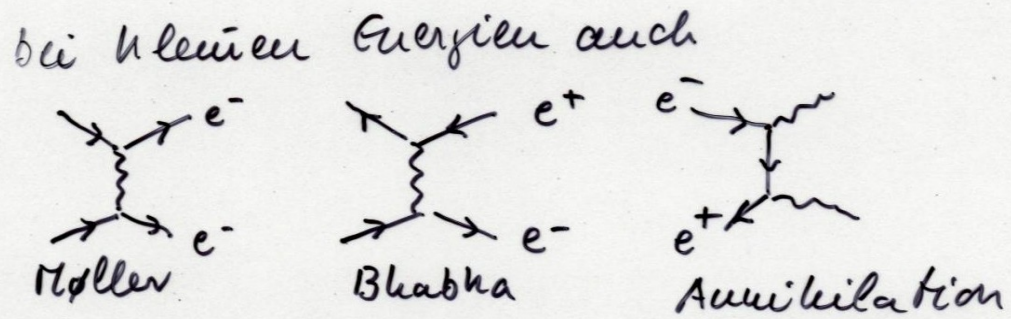


Figure 26.9: Fractional energy loss per radiation length in lead as a function of electron or positron energy. Electron (positron) scattering is considered as ionization when the energy loss per collision is below 0.255 MeV, and as Moller (Bhabha) scattering when it is above. Adapted from Fig. 3.2 from Messel and Crawford, *Electron-Photon Shower Distribution Function Tables for Lead, Copper, and Air Absorbers*, Pergamon Press, 1970. Messel and Crawford use $X_0(\text{Pb}) = 5.82 \text{ g/cm}^2$, but we have modified the figures to reflect the value given in the Table of Atomic and Nuclear Properties of Materials ($X_0(\text{Pb}) = 6.37 \text{ g/cm}^2$).

Photonen

Gesamtabsorptionskoeffizient

$$\sigma_{tot} = \sigma_{ph} + \sigma_c + \sigma_p$$

$$\mu = \mu_{ph} + \mu_c + \mu_p \quad \mu_i = \mu \sigma_i = \frac{N_A \rho}{A} \sigma_i$$

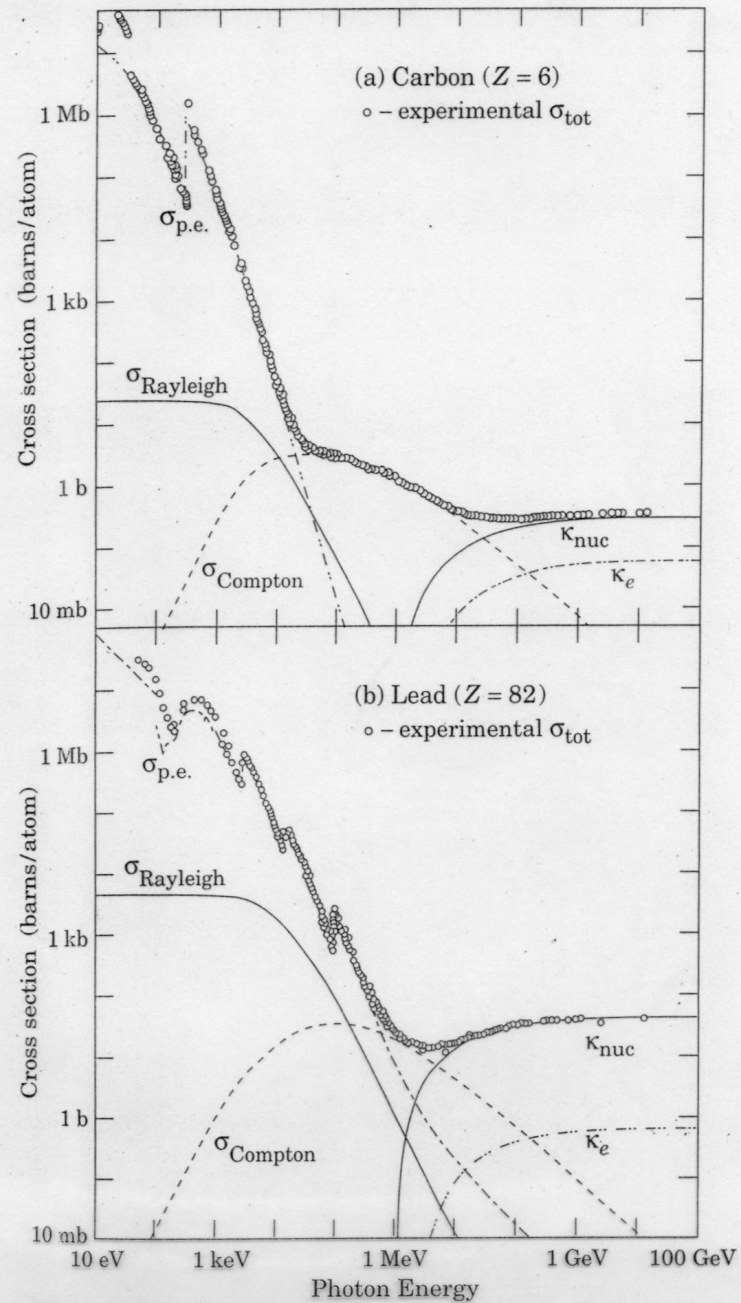


Figure 26.13: Photon total cross sections as a function of energy in carbon and lead, showing the contributions of different

mit wachsender Photon-
Energie wird Paar-
bildung zunehmend
dominant

für Pb über 4 MeV
für H über 70 MeV

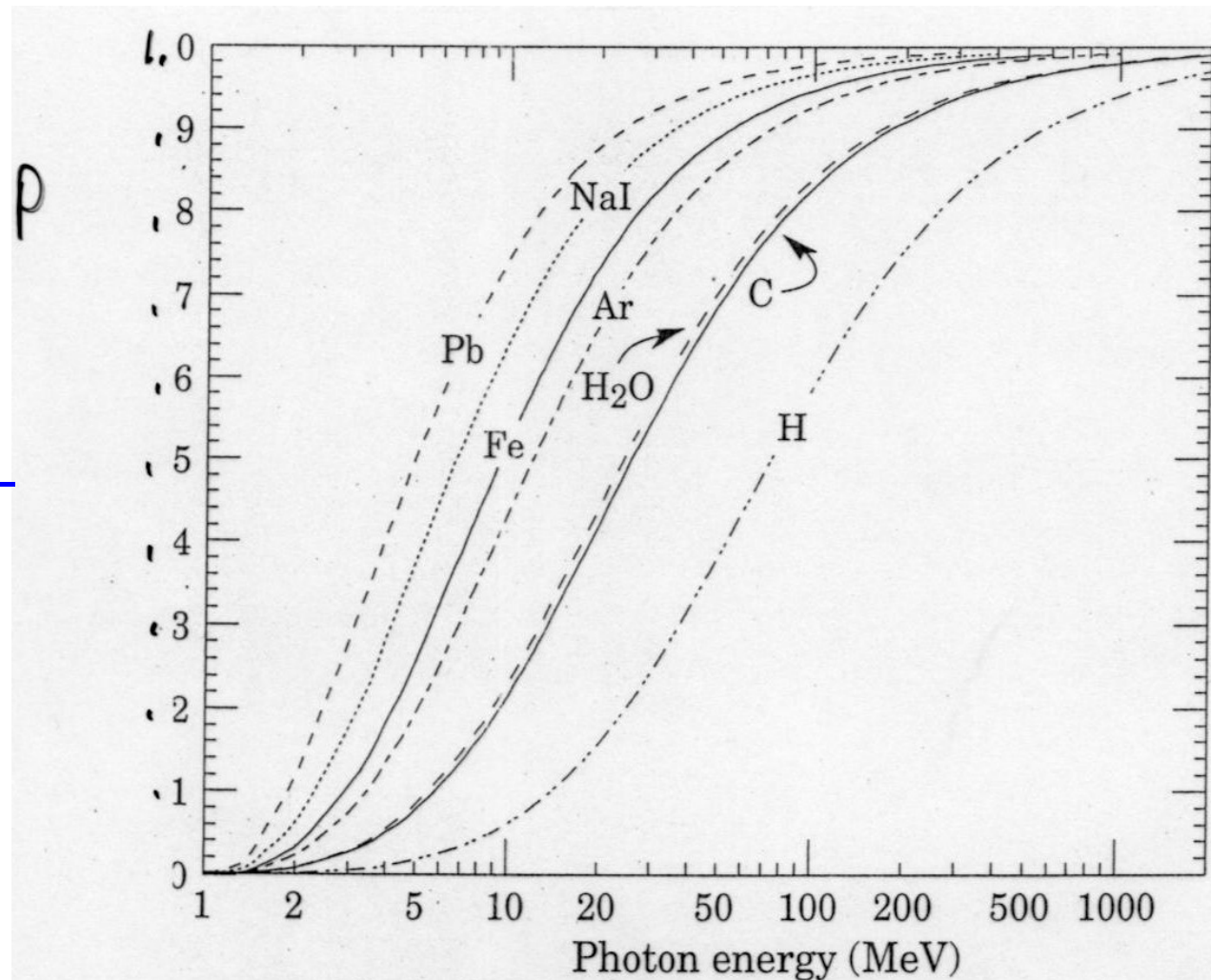


Figure 26.16: Probability P that a photon interaction will result in conversion to an e^+e^- pair. Except for a few-percent contribution from photonuclear absorption around 10 or 20 MeV, essentially all other interactions in this energy range result in Compton scattering off an atomic electron. For a photon attenuation length λ (Fig. 26.15), the probability that a given photon will produce an electron pair (without first Compton scattering) in thickness t of absorber is $P[1 - \exp(-t/\lambda)]$.

Photon Massenabsorptionslänge $\lambda = 1/(\mu/\rho)$

mittlere freie Weglänge

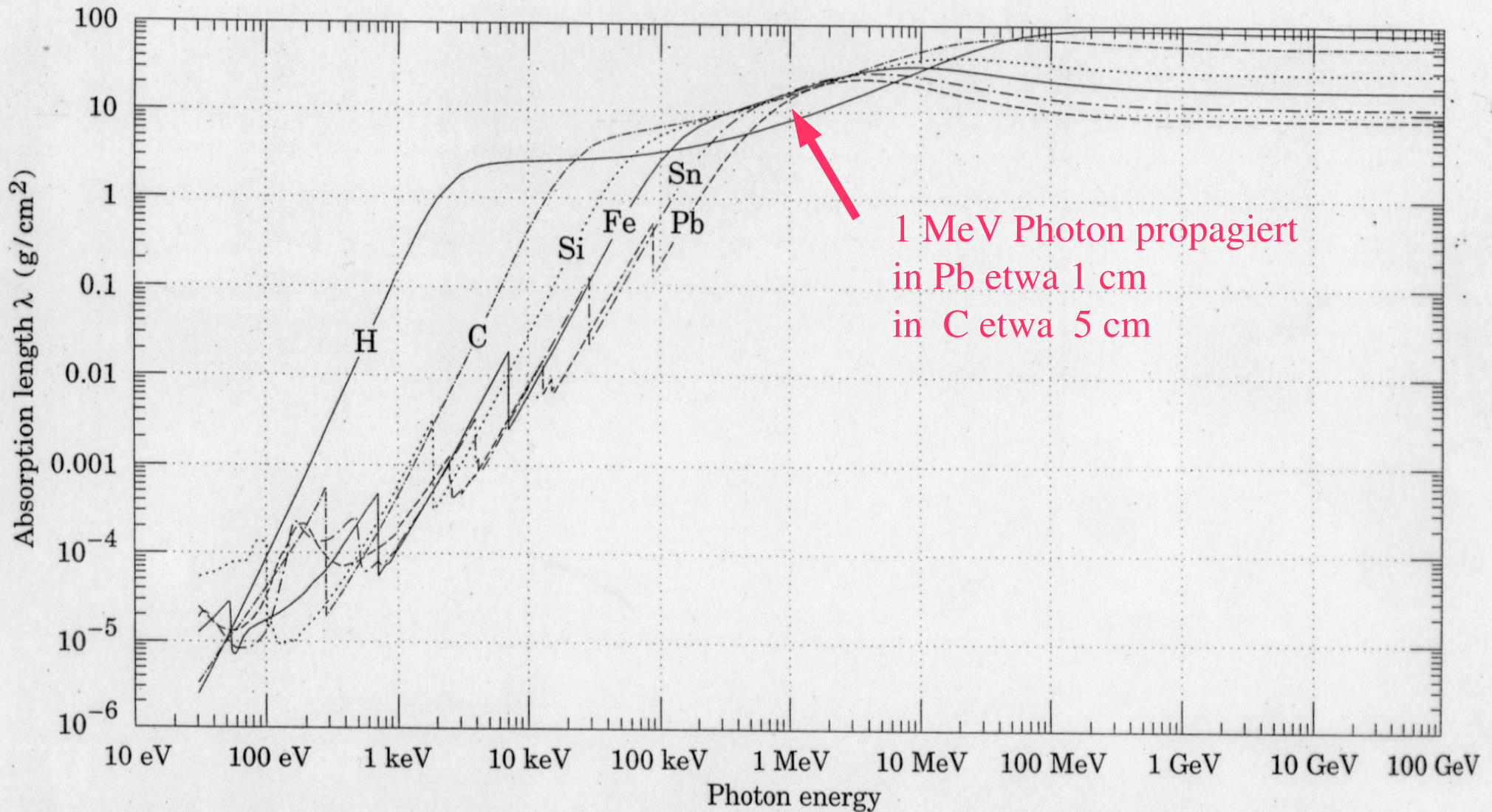
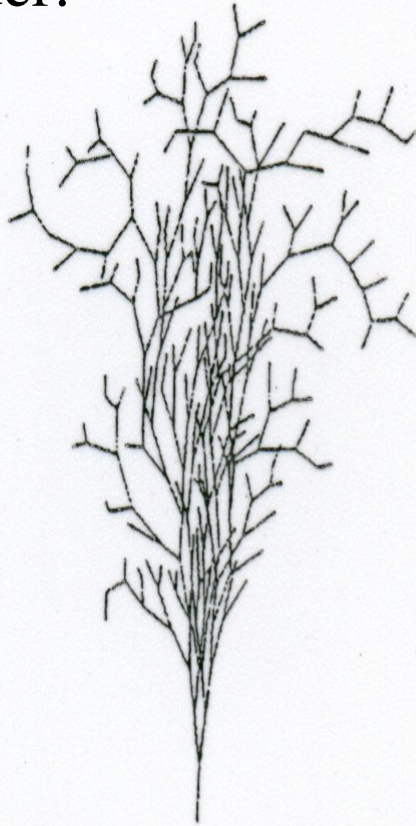


Fig. 26.15: The photon mass attenuation length (or mean free path) $\lambda = 1/(\mu/\rho)$ for various elemental absorbers as a function of photon energy. The mass attenuation coefficient is μ/ρ , where ρ is the density. The intensity I remaining after traversal of thickness t (in mass/unit area) is given by $I = I_0 \exp(-t/\lambda)$. The accuracy is a few percent. For a chemical compound or mixture, $1/\lambda_{\text{eff}} \approx \sum_{\text{elements}} w_Z/\lambda_Z$, where w_Z is the proportion by weight of the element with atomic number Z . The processes responsible for attenuation are given in not Fig. 26.9. Since coherent processes are included, not all these processes result in energy deposition. The data for $30 \text{ eV} < E < 1 \text{ keV}$ are obtained from http://www-cxro.lbl.gov/optical_constants (courtesy of Eric M. Gullikson, LBNL). The data for $1 \text{ keV} < E < 100 \text{ GeV}$ are from <http://physics.nist.gov/PhysRefData>, through the courtesy of John H. Hubbell (NIST).

Elektromagnetischer Schauer:



Betriebsmoden von Gasdetektoren je nach E-Feld

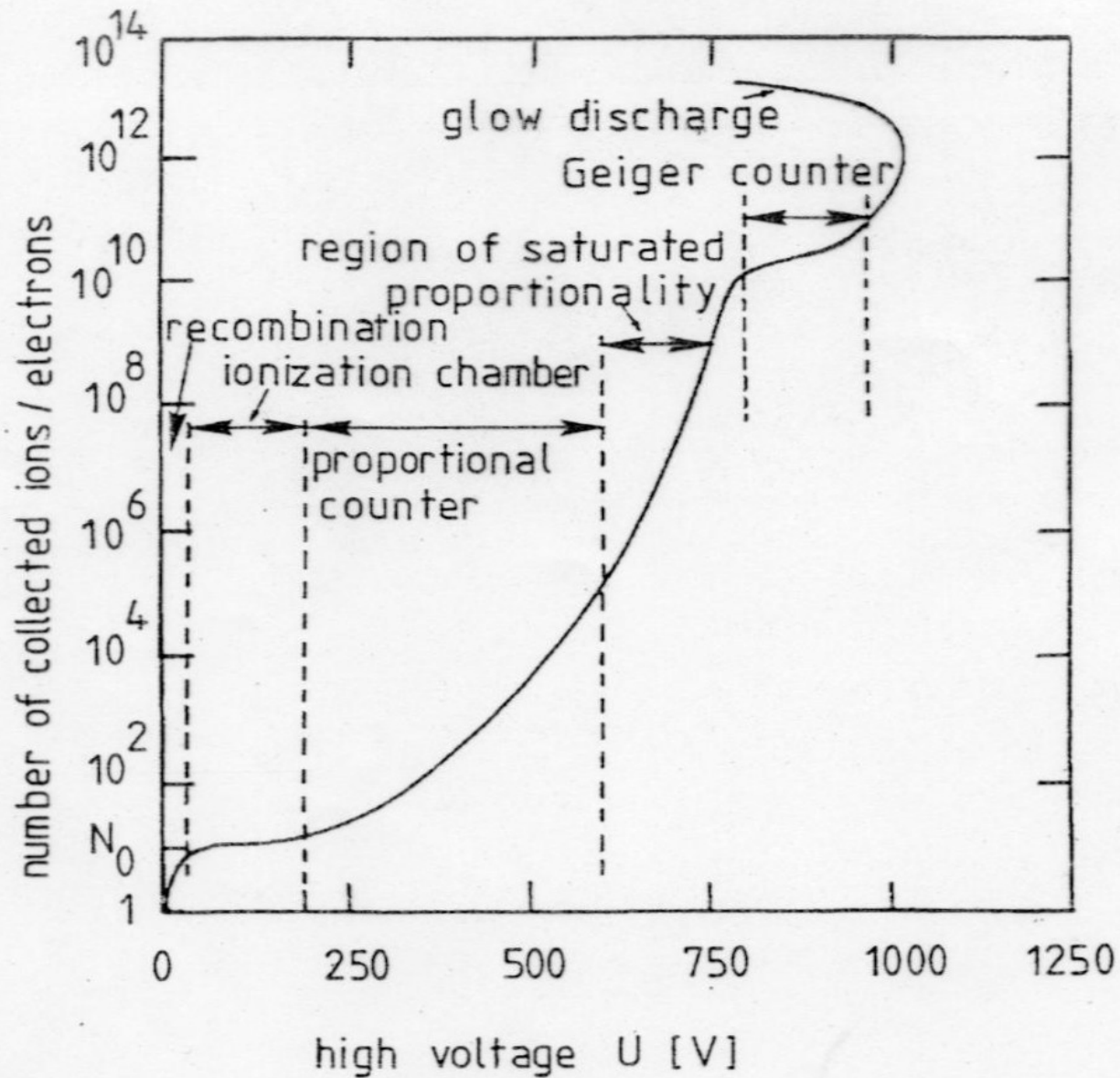


Fig. 4.21. Characterization of the modes of operation of cylindrical gas detectors (after [51]).